Molecularly Annotation of Mouse Avatar Models Derived From Patients With Colorectal Cancer Liver Metastasis

Jingyuan Wang[a,1], Baocai Xing[b,1], Wei Liu[b], Jian Li[a], Xicheng Wang[a], Juan Li[b], Jing Yang[a], Congcong Ji[a], Zhongwu Li[c], Bin Dong[c], Jing Gao*[,a], Lin Shen*[,a]

[a]Key laboratory of Carcinogenesis and Translational Research (Ministry of Education/Beijing), Department of Gastrointestinal Oncology, Peking University Cancer Hospital and Institute, 52 Fucheng Road, Haidian District, Beijing 100142, China.

[b]Key Laboratory of Carcinogenesis and Translational Research (Ministry of Education), Hepatopancreatobiliary Surgery Department I, Peking University Cancer Hospital and Institute, 52 Fucheng Road, Haidian District, Beijing 100142, China.

[c]Department of Pathology, Key Laboratory of Carcinogenesis and Translational Research (Ministry of Education/Beijing), Peking University Cancer Hospital and Institute, 52 Fucheng Road, Haidian District, Beijing 100142, China.

[1] These authors contributed equally to this work.

*Corresponding authors:

Professor Lin Shen, 52 Fucheng Road, Haidian District, Beijing, 100142, China. Tel: +86-10-88196561. Email: shenlin@bjmu.edu.cn;

Professor Jing Gao, 52 Fucheng Road, Haidian District, Beijing, 100142, China. Tel: +86-10-88196747. Email: gaojing_pumc@163.com.

Supplementary figures

Figure S1

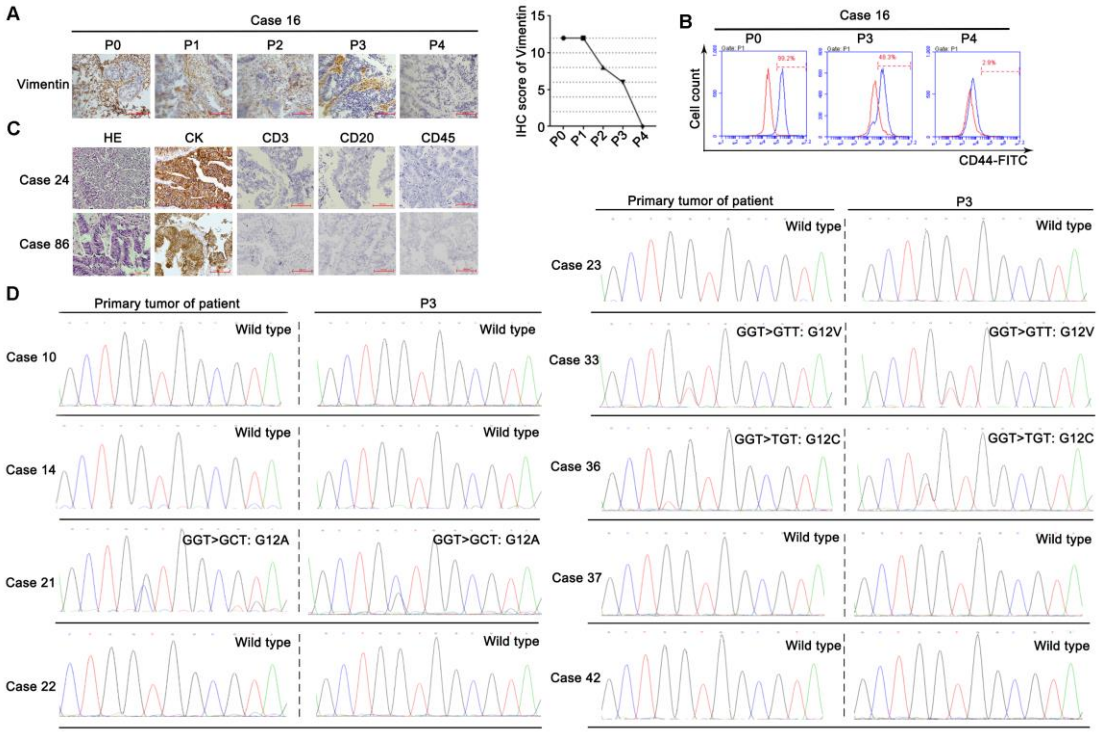

Figure S1. The histopathological and molecular features of PDX models were evaluated during passage. (A) The expression of human vimentin were decreased by IHC staining during passage. Quantification of IHC staining for human vimentin was shown right. **(B)** The expression of human CD44 of CAF cultured *in vitro* decreased by the flow cytometric analysis. **(C)** The histopathological features and leukocyte markers (human CD45, CD20, CD3), as well as human cancer cell marker (CK) were evaluated to confirm that no lymphoma transformation occurred. Positive staining was counted from five randomly selected areas in each slide at ×400 magnification. Scale bars = 100 μm. **(D)** The mutational status of *KRAS* was compared between PDX models and parental tumors, validated by sanger sequencing. No discrepancies

between PDX models and parental tumors were observed in KRAS mutational types (Wild type, G12A, G12V, G12C).

Figure S2

A

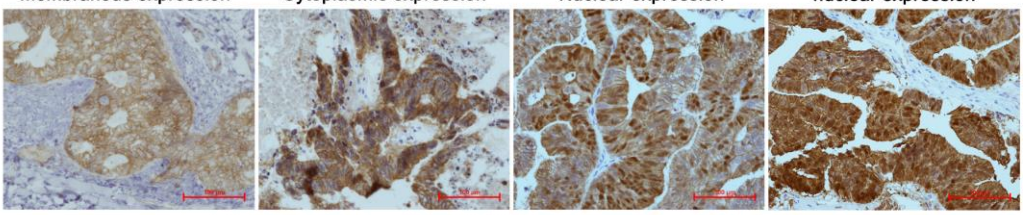

B

β -catenin expression levels in CRLM and CRPT PDX models

		Cytoplasmic expression		Nuclear expression		Membranous expression	
PDX models	Total N	-	+	-	+	-	+
CRLM	56	15	41	29	27	21	35
CRPT	15	5	10	9	6	7	8

Figure S2. Immunohistochemical staining of β-catenin in CRLM and CRPT PDXs. **(A)** Different staining patterns for β-catenin in PDXs: membranous expression, cytoplasmic expression, nuclear expression, nuclear and cytoplasmic β-catenin expression. **(B)** The summary of expression of β-catenin in CRLM and CRPT PDXs. Positive staining was counted from five randomly selected areas in each slide at × 400 magnification. Scale bars = 100 μm.

Figure S3

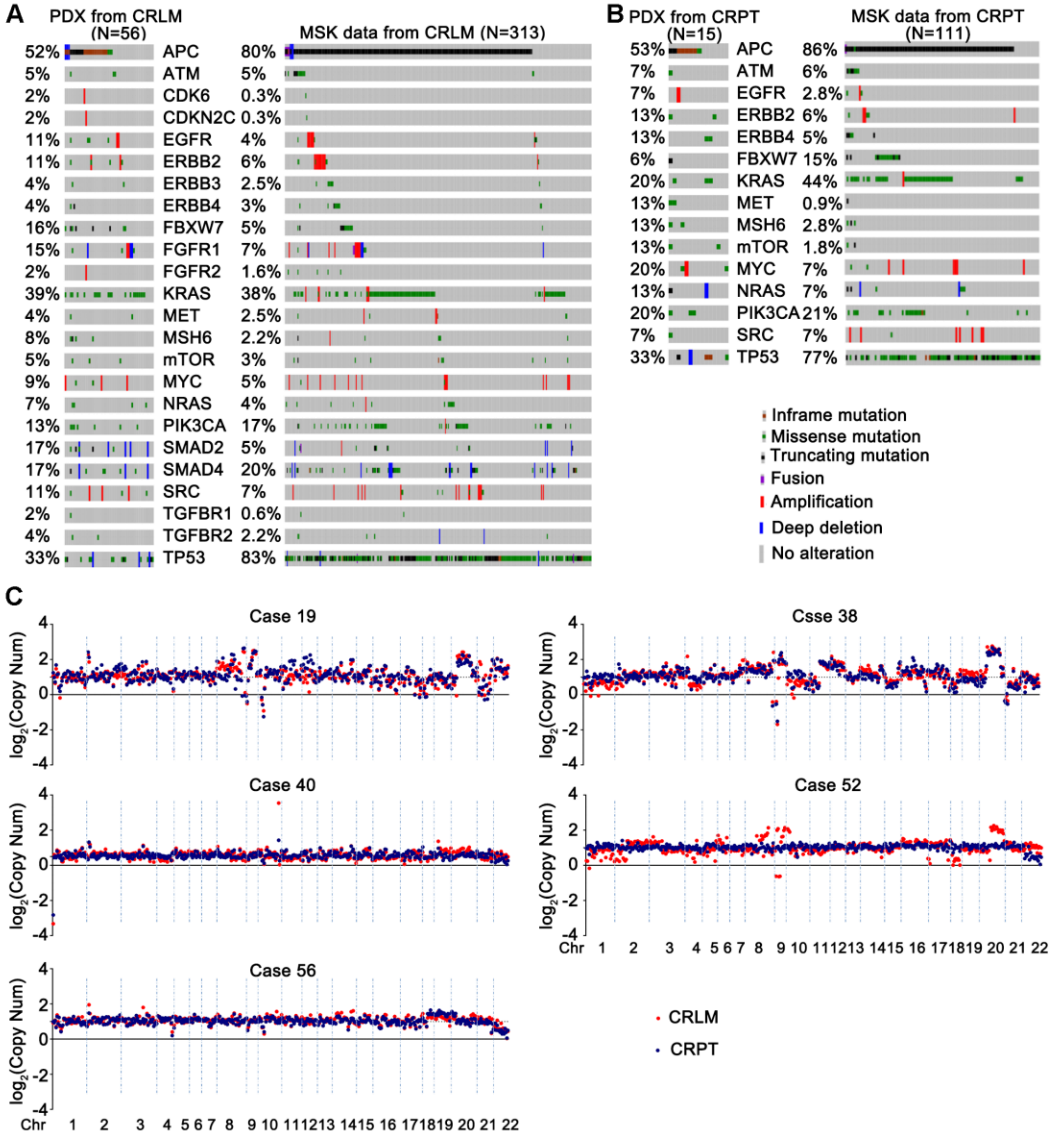

Figure S3. Comparison of genomic alterations in CRLM and CRPT PDXs. **(A-B)** Genomic landscape analysis of genes altered in the PDX and MSK database from liver metastases (A) and primary tumors (B). Red, amplification; Black, truncating mutation; Maroon, inframe mutation; Green, missense mutation; Blue, deletion. **(C)** The copy numbers of five paired PDXs from patients with colorectal cancer liver metastases.

Figure S4

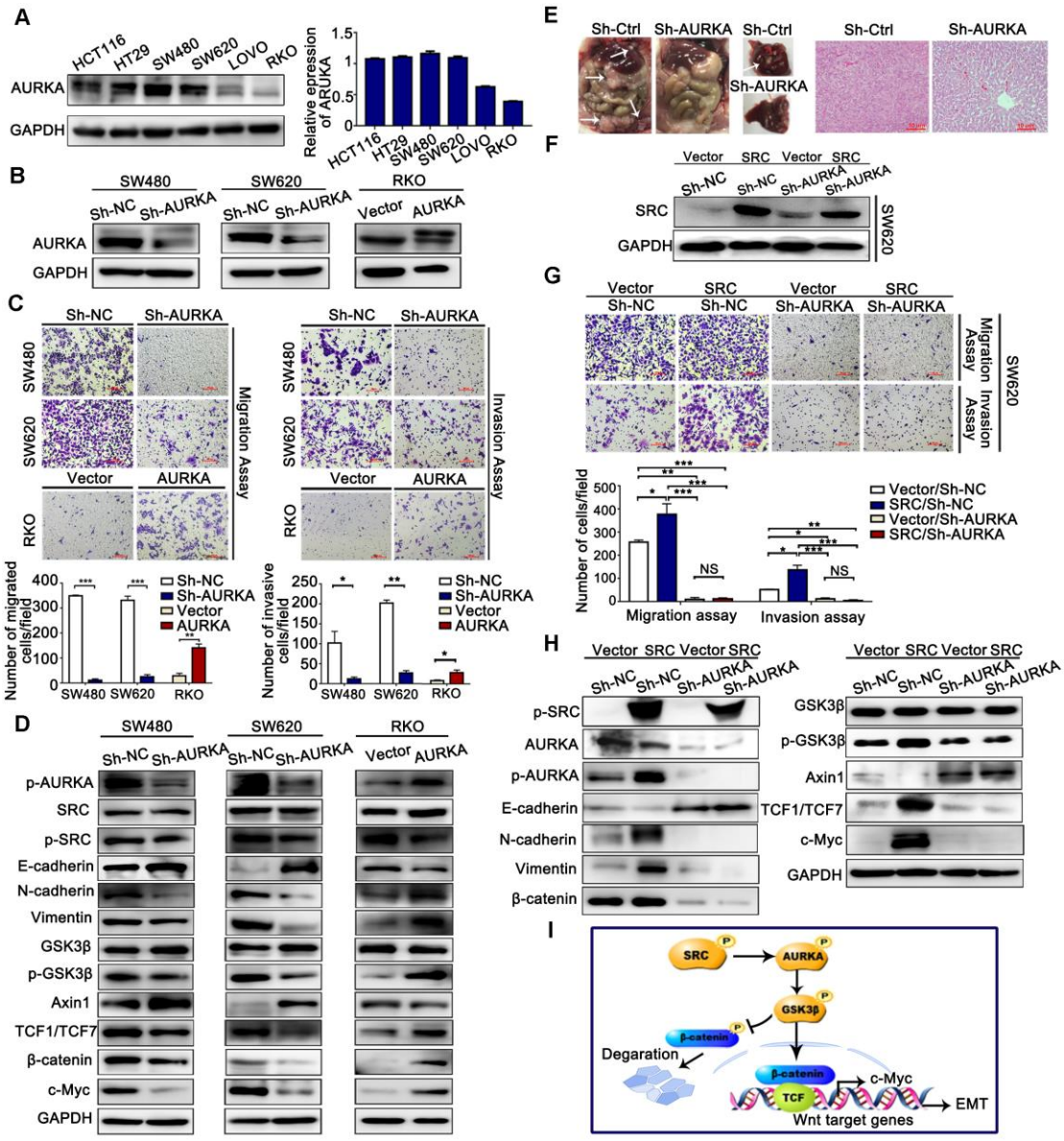

Figure S4. The role of AURKA and SRC in the metastasis of CRC cell lines. **(A)** AURKA expression in six CRC cell lines detected by western-blotting (Left). Images on right shows the protein expression levels of AURKA was quantified by the software Image J (Right). **(B)** Cells transfected with sh-AURKA and AURKA respectively, were detected using western-blotting. **(C)** AURKA suppressed cell migration and invasion detected by Transwell assays. Cells were seeded in upper chamber of insert and the migrated (Left)/invaded (Right) cells were examined after

12~24 h. Data represent the means ± S.D. from three independent experiments. Representative photos of stained cells are shown; scale bar, 100 μm. **(D)** Key pathways related to the metastasis including EMT and wnt signaling pathway were examined by Western-blotting; **(E)** Intraperitoneal injection of SW620/NC and SW620/sh-AURKA cell lines respectively. The inhibition of AURKA decrease metastasis ability of SW620 *in vivo* (Left). Representative H&E stained liver sections containing metastatic foci (Right). Scale bars =10 μm; Arrows: metastatic sites. **(F)** The SRC overexpression and relative control SW620 were incubated with or without AURKA specific shRNA (Sh-AURKA). **(G)** SRC enhanced cancer cell migration and invasion through increasing AURKA expression by Transwell assays. Data represent the means ± S.D. from three independent experiments. Representative photos of stained cells are shown; scale bar, 100 μm. **(H)** Inhibition of AURKA eliminated the SRC enhanced migration and invasion by suppressing SRC-induced wnt signaling pathway and EMT. **(I)** Mechanism diagram of the role of AURKA and SRC in the metastasis of CRC were showed.

Figure S5

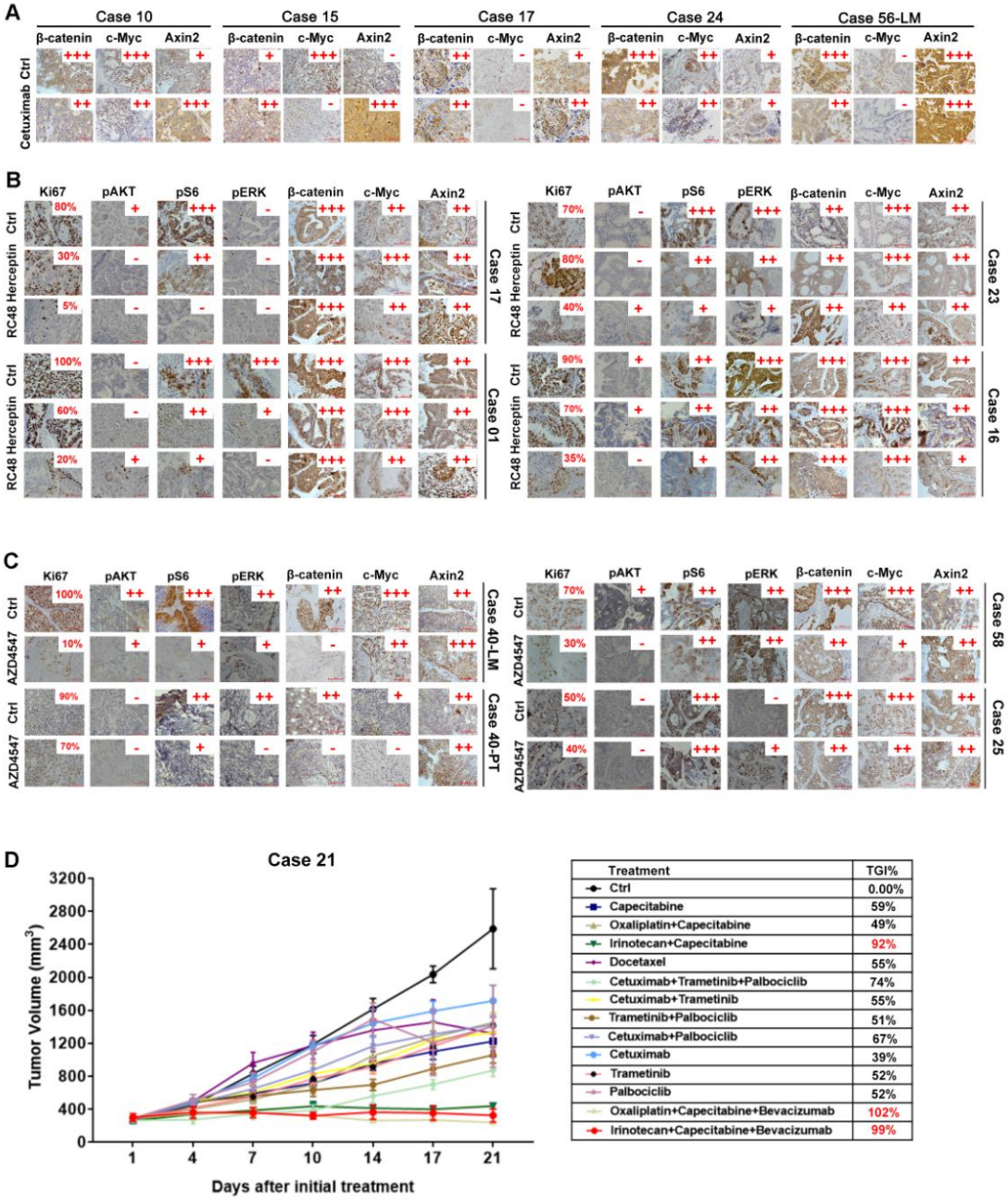

Figure S5. (A) Immunohistochemical staining of xenograft tumor tissues with the indicated antibodies in anti-EGFR therapy. Cetuximab exerted tumor supression activity therapy via the decreased expression of c-Myc and increased expression of Axin2, while no significant change of β-catenin nuclear accumulation. **(B)**

Immunohistochemical staining of xenograft tumor tissues with the indicated antibodies in anti-HER2 therapy. The mechanism of anti-HER2 therapy by RC48 and Herceptin in CRLM PDXs, indicated by the inactivation of PI3K/AKT/mTOR and MAPK signaling pathways, instead of wnt signaling pathway. **(C)** Immunohistochemical staining of xenograft tumor tissues with the indicated antibodies in anti-FGFR2 therapy. The mechanism of anti-FGFR2 therapy in CRLM PDXs by AZD4547, indicated by the inactivation of PI3K/AKT/mTOR and MAPK signaling pathways, instead of wnt signaling pathway. Representative images and quantification of the immunostaining of ki-67, p-AKT, p-S6, p-ERK, c-Myc, Axin 2 and β-catenin were shown. Positive staining was counted from five randomly selected areas in each slide at × 400 magnification. Scale bars = 100 μm. **(D)** PDX with no druggable target was treated by a number of FDA approved drugs. Tumor volumes and proportion of tumor growth inhibition were expressed as means ± S.D. The antitumor activity was depicted by % TGI. TGI = (1-ΔT/ΔC) × 100%, (ΔT = Tumor volume change of the drug-treated group, ΔC = Tumor volume change of the control group on the final day of the study). Tumor volumes and proportion of tumor growth inhibition were expressed as means ± S.D.

Supplementary Tables

Table S1. Patient characteristics and *in vivo* tumorigenicity of CRPT[1] PDXs.

ID	Type of sample	Sex	Age	Stage	Primary site[2]	Pathology[3]	*In vivo* Tumorigenicity[4]
Case 11-PT	Surgery	Male	52	IV	Left side	Good	No
Case 19-PT	Surgery	Male	58	IV	Left side	Good	Yes
Case 31-PT	Surgery	Female	48	IV	Left side	Good	Yes
Case 33-PT	Surgery	Female	63	IV	Left side	Poor	No
Case 38-PT	Surgery	Male	53	IV	Left side	Good	Yes
Case 40-PT	Surgery	Male	38	IV	Left side	Good	Yes
Case 46-PT	Surgery	Female	62	IV	Left side	Poor	No
Case 47-PT	Surgery	Female	49	IV	Right side	Good	No
Case 49-PT	Surgery	Female	28	IV	Left side	Poor	No
Case 51-PT	Surgery	Male	54	IV	Left side	Good	No
Case 52-PT	Surgery	Male	71	IV	Left side	Good	Yes
Case 56-PT	Surgery	Male	28	IV	Left side	Good	Yes
Case 78-PT	Surgery	Male	65	IV	Left side	Good	Yes
Case 81	Biopsy	Male	37	IV	Left side	Good	Yes
Case 82	Biopsy	NA	NA	IV	Left side	Good	No
Case 83	Biopsy	Female	73	IV	Left side	Good	Yes
Case 84	Biopsy	NA	NA	IV	Left side	Poor	Yes
Case 85	Biopsy	Male	72	IV	Right side	Good	Yes
Case 86	Biopsy	Male	43	IV	Right side	Good	Yes
Case 87	Biopsy	Female	60	IV	Right side	Good	Yes
Case 88	Biopsy	Female	36	IV	Right side	Good	Yes
Case 89	Biopsy	Male	54	IV	Right side	Poor	No
Case 90	Biopsy	Male	31	IV	Left side	Poor	No
Case 91	Biopsy	Female	69	IV	Right side	Poor	No
Case 92	Biopsy	Female	53	IV	Left side	Good	Yes
Case 93	Biopsy	Male	NA	IV	Right side	Good	No

[1]CRPT: Colorectal cancer primary tumors.

[2]Left side of colorectum involved left colon and rectum.

[3]Good including well-differentiated and moderately differentiated adenocarcinoma, Poor including poor-differentiated adenocarcinoma, mucinous adenocarcinoma and signet ring cell carcinoma.

[4]*In vivo* tumorigenicity was defined as the successful establishment of P3.

Table S3 The list of 483 genes				
ABCB1	CYP19A1	HRAS	PDK1	TNFRSF14
ABCC1	CYP1A1	HSP90AA1	PHF6	TNFRSF8
ABCC2	CYP1A2	IDH1	PHKA2	TNFSF11
ABCC4	CYP1B1	IDH2	PIGF	TNFSF13B
ABCC6	CYP2A6	IGF1	PIK3CA	TOP1
ABCG2	CYP2B6	IGF1R/IGFR	PIK3CB	TP53
ABL1	CYP2C19	IGF2	PIK3CG	TPMT
ACK1/TNK2	CYP2C8	IGF2R	PIK3R1	TPX2
ACVR1B	CYP2C9	IKBKB	PIK3R2	TRAIL-R1/TNFRSF10A
AKT1	CYP2D6	IKBKE	PKC/PRRT2	TRAIL-R2/TNFRSF10B
AKT2	CYP2E1	IKZF1	PKCγ/PRKCG	TSC1
AKT3	CYP3A4	IL7R	PKCε/PRKCE	TSC2
ALK	CYP3A5	INHBA	PLK1	TSHR
AMER1	CYP4B1	INSR/IR	PPARD	TYMS/TS
APC	DAXX	IRF4	PPP1R13L	TYRO3
AR	DDR1	IRS2	PPP2R1A	U2AF1
ARAF	DDR2	ITK	PRDM1	UBE2I
ARFRP1	DNMT1	JAK1	PRDX4	UGT1A1
ARID1A	DNMT3A	JAK2	PRKAA1	UGT1A9
ARID1B	DOT1L	JAK3	PRKAR1A	UGT2B15
ARID2	DPYD	JUN	PRKCA	UGT2B17
ASXL1	DSCAM	KAT6A	PRKCB	UGT2B7
ATIC	E2F1	KDM5A	PRKDC	UMPS
ATM	EGF	KDM5C	PTCH1	VEGFA
ATP7A	EGFL7	KDM6A	PTEN	VEGFB
ATR	EGFR	KDR/VEGFR	PTK2	VHL
ATRX	EGR1	KEAP1	PTPN11	WEE1
AURKA	EMC8	KIT	PTPRD	WISP3
AURKB	EML4	KLC3	RAC2	WNK3
AXIN1	ENOSF1	KLHL6	RAD50	WT1
AXL	EP300	KMT2A/MLL	RAD51	XPC
B2M	EPH/EPHA1	KMT2B/MLL4	RAF1	XPO1
BAIAP3	EPHA2	KMT2C/MLL3	RARA	XRCC1
BAP1	EPHA3	KMT2D/MLL2	RB1	XRCC4
BARD1	EPHA4	KRAS	RET	YES1

BCL2	EPHA5	LCK	RICTOR	ZAP70
BCL2L2	EPHA7	LIMK1	RMDN2	ZC3HAV1
BCL6	EPHA8	LMO1	RNF43	ZNF217
BCOR	EPHB1	LRP1B	ROCK1	ZNF703
BCORL1	EPHB2	LRP2	RON/MST1R	
BCR	EPHB3	LYN	ROS1	
BIRC5	EPHX1	MAP2K1	RPL13	
BLK	ERBB2/HER2	MAP2K2	RPS6KA1	
BLM	ERBB3	MAP2K4	RPS6KB1	
BRAF	ERBB4	MAP3K1	RPTOR	
BRCA1	ERCC1	MAP4K4	RRM1	
BRCA2	ERCC2	MAP4K5	RUNX1	
BRIP1	ERG	MAPK1	SCF/KITLG	
BRK/PTK6	ESR1/ER	MAPK10	SDHA	
BSG/CD147	ETV1	MAPK14	SDHAF1	
BTK	ETV4	MAPK8	SDHAF2	
C11orf30	ETV5	MAPK9	SDHB	
C18orf56	ETV6	MAPKAPK2	SDHC	
C8orf34	EWSR1	MARK1	SDHD	
CAMK2G	EZH2	MCL1	SETD2	
CAMKK2	FAM46C	MDM2	SF3B1	
CARD11	FANCA	MDM4	SGK1	
CASP8	FANCC	MED12	SHH	
CBFB	FANCD2	MEF2B	SIK1	
CBL	FANCE	MEN1	SKP2	
CBR1	FANCF	MERTK	SLC10A2	
CBR3	FANCG	MET	SLC15A2	
CCND1	FANCL	MITF	SLC22A1	
CCND2	FBXW7	MKNK2	SLC22A16	
CCND3	FCGR3A	MLH1	SLC22A2	
CCNE1	FGF10	MPL	SLC22A6	
CCR4	FGF14	MRE11A	SLCO1B1	
CD19	FGF19	MS4A1	SLCO1B3	
CD22	FGF23	MSH2	SMAD2	
CD274	FGF3	MSH6	SMAD4	
CD33	FGF4	MTDH	SMARCA4	
CD38	FGF6	MTHFR	SMARCB1	
CD3EAP	FGFR1	MTOR	SMO	
CD52	FGFR2	MTRR	SOCS1	

CD74	FGFR3	MUTYH	SOD2	
CD79A	FGFR4	MYC	SOX10	
CD79B	FGR	MYCL1	SOX2	
CDA	FKBP1A	MYCN	SOX9	
CDC73	FLT1	MYD88	SPEN	
CDH1	FLT3	NAT1	SPG7	
CDK1	FLT4	NAT2	SPOP	
CDK12	FOXL2	NCAM1	SRC	
CDK2	FRK	NCF4	SRD5A2	
CDK4	FUBP1	NCOA3	SRMS	
CDK5	FYN	NCOR1	STAG2	
CDK6	FZD7	NEK11	STAT1	
CDK7	GALNT14	NF1	STAT2	
CDK8	GATA1	NF2	STAT3	
CDK9	GATA2	NFE2L2	STAT4	
CDKN1B	GATA3	NFKBIA	STAT5A	
CDKN2A	GCK	NKX2-1	STAT5B	
CDKN2B	GID4	NOS3	STAT6	
CDKN2C	GINS2	NOTCH1	STEAP1	
CEBPA	GNA11	NOTCH2	STK11	
CHEK1	GNA13	NPM1	STK3	
CHEK2	GNAQ	NQO1	STK4	
CHST3	GNAS	NRAS	SUFU	
CIC	GPC3	NTRK1	SULT1A1	
CSNK1A1	GPR124	NTRK2	SULT1A2	
COMT	GRIN2A	NTRK3	SULT1C4	
CREBBP	GSK3B	NUP93	SYK	
CRKL	GSTM1	PAK1	TCF7L1	
CRLF2	GSTM3	PAK3	TCF7L2	
CSF1R	GSTP1	PALB2	TEK	
CSK	GSTT1	PARP1	TET2	
CTCF	H3F3A	PARP2	TGFBR1	
CTLA4	HCK	PAX5	TGFBR2	
CTNNA1	HGF	PBRM1	TK1	
CTNNB1	HIF-1/HIF1A	PDCD1	TMPRSS2	
CYBA	HIST1H3B	PDGFRA	TNF	
CYLD	HNF1A	PDGFRB	TNFAIP3	

Table S4. Clinicopathologic characteristics of CRLM PDX models and patients with CRLM from MSK data set (liver metastases).

Characteristics	Number of cases (%)		*P*
	PDX (N = 56)	MSK (N = 313)	
Age[1]	60 (25–78)	54 (24–86)	**0.24**
Sex			**0.099**
Male	38 (67.9%)	172 (55.0%)	
Female	18 (32.1%)	141 (45.0%)	
Differentiation[2]			**0.298**
Good	46 (82.1%)	185 (59.2%)	
Poor	10 (17.9%)	24 (7.6%)	
NA[3]	/	104 (33.2%)	
Tumor site			**0.816**
Left side[4]	46 (82.1%)	244 (78.0%)	
Right side	10 (17.9%)	62 (19.8%)	
NA	/	7 (2.2%)	
Prior therapy			**0.108**
Neoadjuvant therapy	48 (85.7%)	234 (74.9%)	
No neoadjuvant therapy	8 (14.3%)	79 (25.1%)	
Time to metastasis[5]			**0.118**
synchronous	34 (60.7%)	225 (74.8%)	
metachronous	22 (39.3%)	87 (27.8%)	
NA	/	1 (0.3%)	
KRAS status			**1**
Wild type	35 (62%)	193 (62%)	
Mutation	21 (38%)	120 (38%)	
MSI status			**1**
MSI	1 (1.8%)	5 (1.6%)	
MSS	55 (98.2%)	194 (62.0%)	
NA	/	114 (36.4%)	

[1]Median (range); [2]Good including well-differentiated and moderately differentiated adenocarcinoma, Poor including poor-differentiated adenocarcinoma and mucinous adenocarcinoma.

[3]NA: not applicable; [4]Left side of colorectum involved left colon and rectum. [5]Synchronous liver metastasis was defined as liver metastatic lesions diagnosed before or within 6 months of the primary CRC diagnosis. All others were considered metachronous Liver metastasis. ***P*** was calculated by chi-square test, unpaired two-tailed t-test or one-way analysis of variance separately.

Table S5. Clinicopathologic characteristics of CRPT PDX models and patients with CRLM from MSK data set (primary tissues).

Characteristics	Number of cases (%)		*P*
	PDX (N = 15)	MSK (N = 111)	
Age[1]	40 (36-73)	54 (29–70)	**0.099**
Sex			**0.062**
Male	9 (60.0%)	54 (48.6%)	
Female	5 (33.3%)	57 (51.4%)	
NA[2]	1 (6.7%)	/	
Differentiation[3]			**0.233**
Good	14 (93.3%)	82 (73.9%)	
Poor	1 (6.7%)	19 (17.1%)	
NA	/	10 (9.0%)	
Tumor site			**0.922**
Left side[4]	11 (73.3%)	80 (72.1%)	
Right side	4 (26.7%)	30 (27.0%)	
NA	/	1 (1.0%)	

[1]Median (range); [2]NA: not applicable; [3]Good including well-differentiated and moderately differentiated adenocarcinoma, Poor including poor-differentiated adenocarcinoma and mucinous adenocarcinoma. [4]Left side of colorectum involved left colon and rectum; ***P*** was calculated by chi-square test, unpaired two-tailed t-test or one-way analysis of variance separately.

Table S6. The distribution of Q20 and Q30 in CRLM/PT PDX.

Sample ID	Effective rate(%)	Error rate(%)	Q20 (%)	Q30 (%)	GC content(%)	AT separation	GC separation
Case 01	95.69	0.03	95.8	90.25	49.73	0.05	0.02
Case 03	95.4	0.03	95.92	90.57	49.89	0.01	0.03
Case 05	94.85	0.04	95.98	90.34	49.61	0.08	0.02
Case 07	94.15	0.03	95.89	90.44	49.89	0.01	0.04
Case 10 P0	98.31	0.03	95.77	90.13	49.47	0.14	0.02
Case 10 P1	97.76	0.03	95.96	90.57	49.77	0.11	0.01
Case 10 P2	97.12	0.03	95.9	90.42	49.44	0.08	0.03
Case 10 P3	93.13	0.04	95.76	90.16	50.2	0.05	0.1
Case 11 P3	95.82	0.03	95.69	90.1	49.86	0.03	0.03
Case 12	99.19	0.03	96.58	91.78	49.59	0.26	0.06
Case 13	94.6	0.03	95.83	90.09	48.66	0.09	0.01
Case 14 P0	96.8	0.03	95.66	89.85	49.42	0.11	0.01
Case 14 P1	97.61	0.03	95.88	90.38	49.61	0.15	0.02
Case 14 P2	98.48	0.03	95.73	90.11	49.11	0.15	0.01
Case 14 P3	96.71	0.03	95.77	90.28	49.91	0.11	0
Case 15	99.21	0.03	97.14	92.83	49.12	0.29	0.22
Case 16	96.32	0.03	95.67	89.88	50.02	0.11	0.04
Case 17	98.15	0.03	95.62	89.77	49.49	0.11	0.01
Case 18	97.35	0.03	95.69	89.84	49.15	0.15	0.01
Case 19-LM	99.01	0.03	96.84	92.72	46.17	0.17	0.2
Case 19-PT	98.78	0.03	96.89	92.53	46.2	0.12	0.1
Case 21 P0	99.44	0.03	97.31	93.28	45.11	0.23	0.14
Case 21 P1	97.99	0.02	97.5	93.66	46.36	0.17	0.13
Case 21 P2	95.48	0.02	97.7	94.06	47.91	0.09	0.13
Case 21 P3	95.93	0.02	97.91	94.91	50.93	0.03	0.11
Case 22 P0	99.46	0.03	97.31	93.28	45.59	0.21	0.14
Case 22 P1	99.07	0.03	97.4	93.5	45.64	0.22	0.17
Case 22 P2	99.62	0.03	97.21	93.08	45.66	0.24	0.16
Case 22 P3	97	0.03	97.38	93.41	50.53	0.17	0.22
Case 23 P0	97.65	0.03	95.62	89.82	49.11	0.14	0.05
Case 23 P1	92.05	0.04	95.58	89.8	50.19	0.08	0.07
Case 23 P2	93.35	0.03	95.76	90.2	49.13	0.05	0.07
Case 23 P3	93.82	0.03	95.53	89.71	49.35	0.02	0.06
Case 24	96.68	0.03	95.55	89.63	49.7	0.08	0
Case 25	97.76	0.03	96.79	91.94	49.84	0.18	0.13
Case 27	98.78	0.02	97.48	93.73	50.77	0.26	0.28
Case 28	95.32	0.02	97.77	94.3	51.2	0.08	0.15

Case 29	98.48	0.02	97.63	94.32	50.75	0.15	0.08
Case 30	94.73	0.02	97.09	92.71	52.79	0.02	0.1
Case 33 P0	99.53	0.03	97.42	93.51	45.79	0.23	0.18
Case 33 P1	99.51	0.02	97.5	93.69	45.7	0.19	0.14
Case 33 P2	98.65	0.02	97.62	93.88	46.95	0.17	0.18
Case 33 P3	98.65	0.03	96.91	92.26	50.2	0.23	0.17
Case 35	97.88	0.03	97.32	93.23	50.28	0.21	0.24
Case 36 P0	98.69	0.03	96.89	92.47	45.92	0.13	0.12
Case 36 P1	98.62	0.03	96.62	91.95	45.83	0.16	0.13
Case 36 P2	98.07	0.03	96.72	92.18	45.72	0.1	0.08
Case 36 P3	98.77	0.03	97.36	93.35	49.59	0.23	0.2
Case 37 P0	97.96	0.03	96.79	92.28	46.25	0.11	0.09
Case 37 P1	98.35	0.03	96.75	92.22	46.52	0.16	0.13
Case 37 P2	98.78	0.03	96.89	92.53	46.2	0.12	0.1
Case 37 P3	98.59	0.03	96.75	91.84	49.9	0.19	0.11
Case 38-LM	96.05	0.02	97.61	94.23	48.81	0.06	0.12
Case 38-PT	93.57	0.02	97.74	94.56	48.47	0.02	0.07
Case 40-LM	98.47	0.02	97.93	94.87	49.55	0.22	0.29
Case 40-PT	99.25	0.02	97.64	94.38	49.97	0.15	0.13
Case 41	98.97	0.02	98.36	95.88	47.61	0.16	0.19
Case 42 P0	98.79	0.02	98.22	95.58	46.44	0.2	0.3
Case 42 P1	99.41	0.02	97.99	95.11	45.59	0.15	0.25
Case 42 P2	99.53	0.02	98.06	95.27	45.63	0.2	0.27
Case 42 P3	99.07	0.03	96.66	91.68	50.1	0.2	0.09
Case 45	97.47	0.03	96.82	91.95	50.34	0.13	0.11
Case 48	97.5	0.02	97.88	94.78	50.14	0.06	0.1
Case 49	96.61	0.03	96.69	91.83	51.19	0.08	0.1
Case 50	98.37	0.03	96.69	91.73	49.6	0.23	0.12
Case 52-LM	97.81	0.03	96.85	91.97	50.78	0.17	0.14
Case 52-PT	98.66	0.03	96.09	90.69	51.69	0.15	0.07
Case 53	98.91	0.02	97.64	94.31	49.91	0.18	0.16
Case 54	98.22	0.03	97.03	92.62	50.08	0.16	0.09
Case 55	98.5	0.02	97.87	94.74	50.19	0.14	0.14
Case 56-LM	98.99	0.03	96.77	92.15	49.76	0.22	0.08
Case 56-PT	98.73	0.03	96.81	92.2	50.04	0.2	0.09
Case 58	98.87	0.02	97.78	94.57	50.22	0.15	0.13
Case 59	98.06	0.02	97.29	93.33	50.95	0.2	0.23
Case 61	99.01	0.02	97.44	93.65	50.3	0.24	0.25
Case 62	97.07	0.03	97.38	93.27	50.27	0.1	0.08
Case 63	98.97	0.02	97.41	93.58	49.78	0.25	0.23

Case 65	96.35	0.02	97.63	94.03	51.36	0.16	0.21
Case 66	98.23	0.02	97.42	93.6	51	0.2	0.23
Case 68	97.44	0.02	97.54	93.84	50.89	0.19	0.22
Case 69	98.45	0.02	97.38	93.55	50.69	0.22	0.21
Case 70	98.14	0.02	98.4	95.97	47.59	0.16	0.22
Case 71	98.21	0.02	97.83	94.64	48.87	0.16	0.19
Case 72	98.77	0.02	97.55	94.12	50.14	0.19	0.1
Case 74	98.88	0.03	97.24	93.53	47.65	0.19	0.18
Case 77	98.67	0.03	97.33	93.66	50.78	0.16	0.06
Case 79	97.78	0.03	97.23	92.72	51.34	0.15	0.15
Case 80	99.33	0.02	98.18	95.52	47.61	0.21	0.22
Case 31-PT	99.28	0.02	97.74	94.27	45.72	0.16	0.22
Case 78-PT	99.57	0.02	97.4	93.6	45.28	0.16	0.21
Case 81	98.81	0.02	97.82	94.39	46.74	0.07	0.2
Case 83	99.28	0.02	97.45	93.66	46.48	0.16	0.25
Case 84	99.48	0.02	97.53	93.84	46.29	0.17	0.27
Case 85	99.2	0.02	97.53	93.81	46.91	0.17	0.27
Case 86	96.76	0.02	97.75	94.29	46.56	0.11	0.22
Case 87	99.01	0.02	97.65	94.06	46.94	0.13	0.26
Case 88	98.78	0.02	97.6	93.99	46.89	0.11	0.25
Case 92	99.49	0.03	97.36	93.38	45.47	0.24	0.18

Supplementary Methods

Antibodies

The following antibodies were purchased from Cell Signaling Technology (Boston, Massachusetts, USA): p-AKT (#4060), p-S6 (#4858), p-ERK (#2947), HER2 (#4290), FGFR2 (#23328), EGFR (#2085), MET (#8198), p-AURKA (#2914), SRC (#2109), p-SRC (#6943), Vimentin (#5741), E-cadherin (#14472), N-cadherin (#13116), β-catenin (#8480), GSK-3β (#12456), p-GSK-3β (#5558), Axin1 (#2074), TCF1/TCF7 (#2203), GAPDH (#5174); The Ki-67 antibody (#ZM-0167), CD3 (#ZM-0417), CD45 (#13917) and CK (#ZM-0069) were purchased from ZSGB-BIO (Beijing, China); Human vimentin (#790-2917) was purchased from Ventana (Tucson, AZ, USA); AURKA (#ab13824), CD20 (#ab78237), Axin2 (#ab32197) and c-Myc (#ab32072) were purchased from abcam (Cambridge, UK); CD44-FITC (#11-0441-81) and IgG1-FITC (#11-4714-81) was purchased from eBioscience (Vienna, Austria).

Administration methods of all the drugs for tumor xenograft studies

The doses of drug used for PDX models were given as followed: RC-48 (RemeGen, Ltd., Yantai, Shandong, China), 5 mg/kg once a week by intravenous injection; Herceptin (Hoffman-La Roche Ltd, Basel, Switzerland), 10 mg/kg once a week by intravenous injection; Cetuximab (Merck KGaA, Darmstadt, Germany), 5 mg/kg twice a week by intraperitoneal injection; AZD4547 (Selleck Chemicals, Houston, TX, USA), 12.5 mg/kg daily by oral gavage; 5-Fluorouracil (Tianjin Jinyao Amino Acid Co., Ltd, Tianjin, China), 10 mg/Kg twice a week by intraperitoneal

injection; Irinotecan (Jiangsu Hengrui Medicine Co., Ltd, Jiangsu, China), 20 mg/kg twice a week by intraperitoneal injection; Leucovorin (Nanjing Chia Tai-Tian Qing Pharmaceutical Co., Ltd, Jiangsu, China), 20 mg/kg twice a week by intravenous injection; Capecitabine (F. Hoffmann-La Roche Co., Ltd, Basel, Switzerland), 180 mg/kg daily by oral gavage; Oxaliplatin (Sanofi Genzyme, Cambridge, MA, USA), 5 mg/kg twice a week by intraperitoneal injection; Bevacizumab (F. Hoffmann-La Roche Co., Ltd, Basel, Switzerland), 5 mg/kg twice a week by intraperitoneal injection.

Gene variant calling and data analysis

The clean reads of all samples were outputted finally with Q20 >90% and Q30 > 85% (Table S6), after cleaning the sequencing adapters and low-quality reads. Then, these reads were matched to the human reference hg19 genome using the Burrows-Wheeler Aligner (BWA) [1]. The original BAM files were sorted using sambamba and remove duplicate reads using samblaster [2, 3]. According to the results of the alignment, the coverage of the target region was over 99%, and the mapping rate was >95%. The variants were called using muTect and VarScan2, for SNP and indel mutations respectively [4, 5]. CNV analysis was performed by ExomeCNV. A neutral copy number for each exon for each gene was established using normal lymphocyte samples. Then, they were functionally annotated with Annovar software. ANNOVAR with information from the COSMIC (http://cancer.sanger.ac.uk/cosmic) and ClinVar (https://www.ncbi.nlm.nih.gov/clinvar/) databases was used for functional annotation of variants [6]. The subsequent filter to identify the candidate genetic alterations as

follows: 1) Retain the variations in the exonic or splicing region, which are more likely to affect the protein function. 2) Remove the SNPs of the single-base repeat region to avoid errors. 3) Remove the mutation sites: depth≤4, mutation abundance≤5% (Avoid false positive due to noise generated by low depth). 4) Remove germline mutations (SAO=1) in SAOdbSNP147, and variant with mutant allele frequency (MAF) >0.005 in the 1,000 Genomes database and the Exome Aggregation Consortium. 5) Remove synonymous mutations. 6) Retain the nonsynonymous SNVs and indels if the functional predictions by SIFT and Polyphen2, which might indicate the alterations are not benign. Genes with high frequency were selectively validated by Sanger sequencing to confirm the mutation (data not shown).

Plasmid construction/transfection

pcDNA3.1 plasmids expressing His-tagged AURKA and SRC were provided by ViGene Biosciences (Rockville, MD, USA). Plasmids were transfected into cells with Lipofectamine 3000. Lentiviral systems for knockdown of AURKA were provided by GenePharma (Suzhou, China) and were infected into cells following the provider's instructions. Interference sequences used were shown as followed:

Control: 5'-TTCTCCGAACGTGTCACGT-3';

AURKA:5'-GGTCTTGTGTCCTTCAAATTC-3';

Transwell assays

Cell migration and invasion assays were performed in 24-well CIM plates with or without Matrigel Basement Membrane Matrix (BD Biosciences) as described

previously [7]. The number of cells permeating septum was counted in five random microscopic fields. The average number of cells in five fields was calculated, which represented the ability of cells to migrate and invade. All values are represented as means ± S.D.

Cancer-associated fibroblast (CAF) culture

The tumor specimens were obtained from patients with CRLM or PDX models. The fresh tumor specimens were cut into 1-mm^3 -sized pieces and cultured in high glucose (H-DMEM) supplemented with 15% FBS and 1% penicillin and streptomycin. The medium was replaced every 3 days after the initial plating. When adherent fibroblast-like cells appeared, the cells were collected for flow cytometry. CAFs were stained with monoclonal antibodies against CD44 (FITC-conjugated). FITC-IgG1 were used as the isotype control.

Western-blotting

The extraction of total protein from cell pellets was performed as previously described [7]. Proteins were visualized using ECL plus Western Blotting Detection Reagents (GE Healthcare). The protein expressions were quantified and normalized by Image J software.

***In vivo* metastasis assay**

SW620/sh AURKA and SW620/sh-NC cell lines (5×10^6 in 100 μL PBS) were injected intraperitoneally into 6-week-old female NOD/SCID mice (N = 5 mice/group), and on the indicated day, the mice were killed and photographed. All the liver tissues were embedded in paraffin, followed by HE and IHC staining. All animal

experiments were performed according to the animal experimental guidelines of Peking University Cancer Hospital.

References:

1. Li H, Durbin R. Fast and accurate long-read alignment with Burrows-Wheeler transform. Bioinformatics. 2010; 26: 589-95.
2. Faust GG, Hall IM. SAMBLASTER: fast duplicate marking and structural variant read extraction. Bioinformatics. 2014; 30: 2503-5.
3. Li H, Handsaker B, Wysoker A, Fennell T, Ruan J, Homer N, et al. The Sequence Alignment/Map format and SAMtools. Bioinformatics. 2009; 25: 2078-9.
4. Cibulskis K, Lawrence MS, Carter SL, Sivachenko A, Jaffe D, Sougnez C, et al. Sensitive detection of somatic point mutations in impure and heterogeneous cancer samples. Nat Biotechnol. 2013; 31: 213-9.
5. Koboldt DC, Zhang Q, Larson DE, Shen D, McLellan MD, Lin L, et al. VarScan 2: somatic mutation and copy number alteration discovery in cancer by exome sequencing. Genome Res. 2012; 22: 568-76.
6. Wang K, Li M, Hakonarson H. ANNOVAR: functional annotation of genetic variants from high-throughput sequencing data. Nucleic Acids Res. 2010; 38: e164.
7. Wang J, Liu Z, Wang Z, Wang S, Chen Z, Li Z, et al. Targeting c-Myc: JQ1 as a promising option for c-Myc-amplified esophageal squamous cell carcinoma. Cancer Lett. 2018; 419: 64-74.